J. Fluid Mech. (1974), *vol.* 62, *part* 3, *pp.* 539–551
Printed in Great Britain

Prediction of laminar flow and heat transfer in helically coiled pipes

By S. V. PATANKAR, V. S. PRATAP AND D. B. SPALDING

Department of Mechanical Engineering, Imperial College, London

(Received 27 May 1973)

A calculation procedure for three-dimensional parabolic flows is applied to predict the velocity and temperature fields in helically coiled pipes. The curvature produces a secondary flow and causes departures from the symmetric velocity profile of Poiseuille flow. Predictions are presented of flow and heat transfer in the developing and fully developed regions. Comparisons of the developing and fully developed velocity profiles with experimental data exhibit good agreement. The development of the wall temperature for the case of axially uniform heat flux with an isothermal periphery has been compared with experimental data and the agreement is good. Predictions for fully developed temperature profiles and heat-transfer coefficients also exhibit good agreement with experimental data. Effects of the Dean number on the friction factor and heat transfer are presented.

1. Introduction

1.1. *The problem considered*

Flow and heat transfer in curved pipes are of importance in the heating and cooling coils used in heat exchangers and refrigeration equipment. The flow in curved pipes is characterized by a secondary flow in a cross-sectional plane normal to the main flow (figure 1), the nature of which depends upon the Dean number $K = Re\ (a/R)^{\frac{1}{2}}$ (a being the radius of the pipe, R its radius of curvature and Re the Reynolds number). The centrifugal forces act at right angles to the main direction of flow, so that the profile of axial velocity is distorted from the symmetric profile of Poiseuille flow; the point at which the velocity has its peak is shifted to the outside.

In the present study, the parabolic differential equations governing three-dimensional flow are solved by the procedure of Patankar & Spalding (1972). The present study has been limited to laminar uniform-property flows; extensions to turbulent and non-Newtonian flows are in progress.

1.2. *Past work*

The literature on laminar flow and heat transfer in curved pipes is quite extensive; however, most of the investigations have been restricted to the 'fully developed' situation in which the pattern of fluid flow and heat transfer remains unchanged from one section to the next. Dean (1927) was one of the first researchers in this

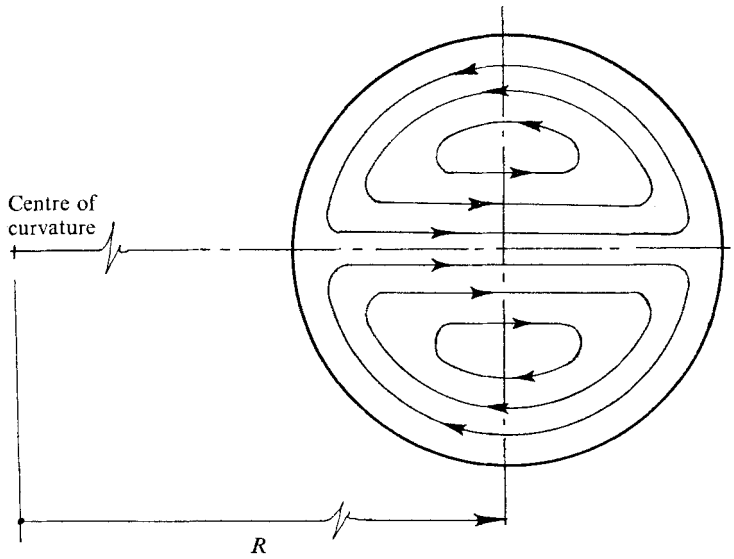

FIGURE 1. Secondary flow pattern.

area; using a perturbation technique, he analysed the secondary flow field as a deviation from Poiseuille flow. Subsequent publications have been summarized by Ito (1970). Mori & Nakayama (1965) solved the governing equations by integral methods, subdividing the flow pattern into a core and a boundary-layer region. A similar analysis was performed by Ito (1970). McConalogue & Srivastava (1968) used a Fourier-series method to solve the governing differential equations for fully developed flow in a curved tube for Dean numbers ranging between 16·6 and 100. Akiyama & Cheng (1971) predicted the fully developed flow and heat-transfer characteristics by solving the finite-difference equations for the vorticity, stream function, axial velocity and temperature.

There have been very few investigations in the developing region of flow and temperature fields. Austin (1971) studied the hydrodynamic entrance region, experimentally. The thermal entry region was studied theoretically by Dravid (1971), who assumed the fully developed velocity profiles of Mori & Nakayama (1965) and employed a finite-difference method to solve the energy equation. These authors also presented experimental data on wall temperatures and Nusselt numbers in the developing and fully developed regions.

1.3. *Present work*

The present study concerns the developing 'entry' flow, both hydrodynamic and thermal, in helically coiled pipes; the finite-difference method of Patankar & Spalding (1972) is used to compute the flow and temperature distributions, section-by-section along the pipe; the fully developed flow appears as the solution for the sections which are remote from the entrance. Comparisons are made with the experimental velocity profiles and friction factors of Ito (1970), Mori & Nakayama (1965) and Austin (1971). The fully developed and developing

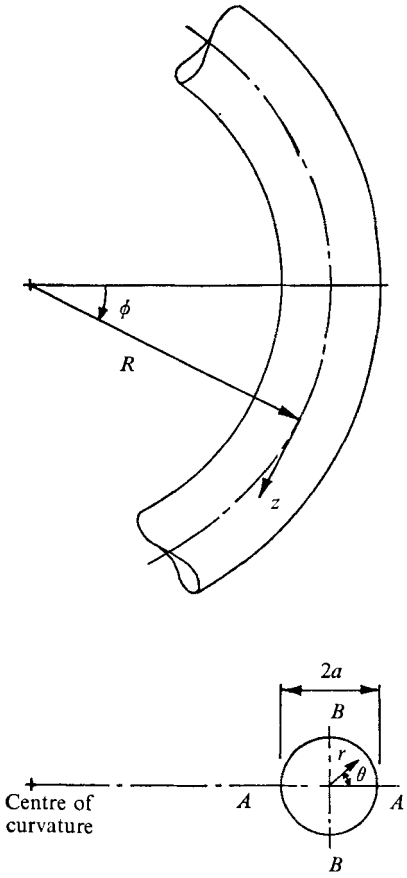

FIGURE 2. The geometry considered.

temperature fields and heat-transfer rates are compared with the experimental data of Mori & Nakayama (1965) and Dravid (1971). Only large curvature ratios ($R/a \geqslant 15$) have been considered in this investigation.

1.4. *Outline of the paper*

The calculation procedure, which is a finite-difference marching technique, is described briefly in §2. The results of the computations and comparisons with experimental data are presented in §3. Section 4 discusses possible further developments.

2. Mathematical statement of the problem

2.1. *The geometry and governing differential equations*

The physical situation, illustrated in figure 2, may be conveniently described in cylindrical polar (r, θ, z) co-ordinates. The fluid properties, namely viscosity, density and specific heat, have been assumed to be uniform, although their variation could have been incorporated easily. The flow is treated as 'parabolic',

i.e. as being of the 'boundary-layer' variety; this means that heat conduction and viscous action in the z direction are neglected.

The governing partial differential equations are the continuity equation

$$\frac{1}{r}\frac{\partial}{\partial r}(rv_r)+\frac{1}{r}\frac{\partial v_\theta}{\partial \theta}+\frac{\partial v_z}{\partial z}=0, \tag{1}$$

the r momentum equation

$$\rho\left[\frac{1}{r}\frac{\partial}{\partial r}(rv_rv_r)+\frac{1}{r}\frac{\partial}{\partial \theta}(rv_rv_\theta)+\frac{1}{r}\frac{\partial}{\partial z}(rv_rv_z)\right]$$
$$=-\frac{\partial p}{\partial r}+\frac{\rho v_\theta^2}{r}+\mu\left[\frac{\partial}{\partial r}\left(\frac{1}{r}\frac{\partial}{r}(rv_r)\right)+\frac{1}{r^2}\frac{\partial^2 v_r}{\partial \theta^2}-\frac{2}{r^2}\frac{\partial v_\theta}{\partial \theta}\right]+\frac{\rho v_z^2}{R}\cos\theta, \tag{2}$$

the θ momentum equation

$$\rho\left[\frac{1}{r}\frac{\partial}{\partial r}(rv_\theta v_r)+\frac{1}{r}\frac{\partial}{\partial \theta}(v_\theta v_\theta)+\frac{1}{r}\frac{\partial}{\partial z}(rv_\theta v_z)\right]$$
$$=-\frac{1}{r}\frac{\partial p}{\partial \theta}-\frac{v_rv_\theta}{r}+\mu\left[\frac{\partial}{\partial r}\left(\frac{1}{r}\frac{\partial}{\partial r}(rv_\theta)\right)+\frac{1}{r^2}\frac{\partial^2 v_\theta}{\partial \theta^2}+\frac{2}{r^2}\frac{\partial v_r}{\partial \theta}\right]-\frac{\rho v_z^2}{R}\sin\theta, \tag{3}$$

the z momentum equation

$$\rho\left[\frac{1}{r}\frac{\partial}{\partial r}(rv_zv_r)+\frac{1}{r}\frac{\partial}{\partial \theta}(v_zv_\theta)+\frac{1}{r}\frac{\partial}{\partial z}(rv_zv_z)\right]=-\frac{\partial \bar{p}}{\partial z}+\mu\left[\frac{1}{r}\frac{\partial}{\partial r}\left(r\frac{\partial v_z}{\partial r}\right)+\frac{1}{r^2}\frac{\partial^2 v_z}{\partial \theta^2}\right] \tag{4}$$

and the energy equation

$$\rho\left[\frac{1}{r}\frac{\partial}{\partial r}(rv_rT)+\frac{1}{r}\frac{\partial(v_\theta T)}{\partial \theta}+\frac{1}{r}\frac{\partial}{\partial z}(rv_zT)\right]=\frac{\mu}{Pr}\left[\frac{1}{r}\frac{\partial}{\partial r}\left(r\frac{\partial T}{\partial r}\right)+\frac{1}{r^2}\left(\frac{\partial^2 T}{\partial \theta^2}\right)\right], \tag{5}$$

where (v_r, v_θ, v_z) is the fluid velocity and ρ and μ its density and viscosity. Pr is the Prandtl number.

A feature of these equations which deserves especial note is that a single pressure $\bar{p}$ is supposed to prevail at each cross-section in the z momentum equation (4); but in the r and θ momentum equations (2) and (3), the pressure p is allowed to vary over the cross-section. This inconsistency, which is a necessary condition for the differential equations to be soluble by a marching technique, has been discussed in Patankar & Spalding (1972) and Caretto, Curr & Spalding (1971); it does not lead to significant error when the Reynolds number is high.

2.2. *Solution procedure*

The above equations, with appropriate boundary conditions, are solved by a finite-difference procedure which we need describe here only in outline, a complete account being given in Patankar & Spalding (1972). The main steps necessary to deduce the flow properties at one pipe cross-section from those at a section immediately upstream are as follows.

(i) The pressure distribution (both $\bar{p}$ and p) at the downstream section is guessed.

(ii) The r, θ and z momentum equations are then solved to get a first approximation to the velocity profile at the downstream section.

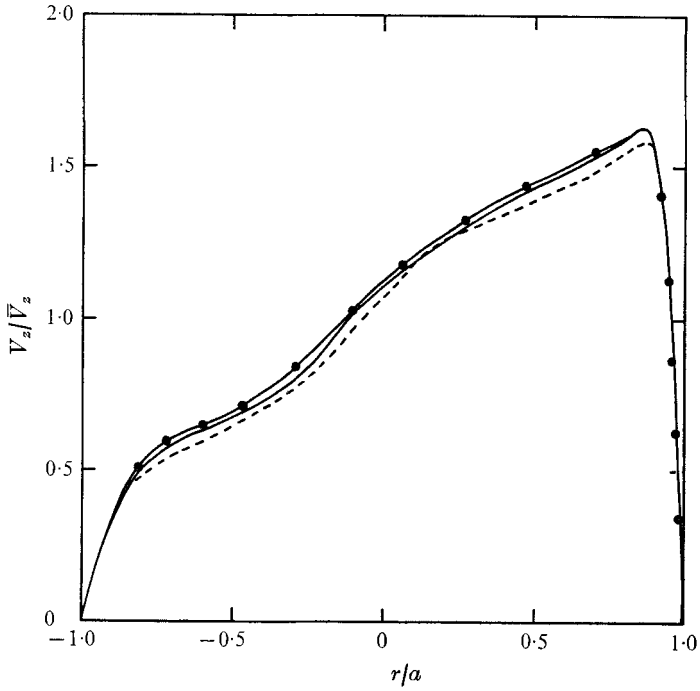

FIGURE 3. Effect of grid size at a Dean number of 800 and radius ratio R/a of 16·4. The velocity profiles are along the plane AA; $\bar{V}_z$ is the cross-sectional average of V_z. Grids: —●—, 18 × 12, non-uniform; ——, 16 × 12, non-uniform; – – –, 12 × 12, non-uniform.

(iii) The mean pressure $\bar{p}$ and the axial velocity are thereupon corrected so as to ensure that the mass flow rate through the downstream section is the same as that through the upstream section.

(iv) Since the cross-stream velocities do not satisfy the continuity equation locally, an equation is solved for corrections to the pressure field (p) and the cross-stream velocities are corrected accordingly.

(v) The energy equation is solved so as to provide the temperature distribution at the downstream station.

(vi) A new downstream station is chosen and steps (i)–(v) are repeated.

3. Results and discussions

3.1. *Computational details*

In the computations from which the following results were derived, the finite-difference grid possessed 15 intervals in the r direction and 11 intervals in the θ direction; the grid covered only a semi-circular sector because the flow must be symmetric about a diameter passing through the axis of the helix. The grid spacing was uniform in the θ direction; in the r direction the grid lines were more closely spaced near the wall than near the centre. That the 15 × 11 grid gave sufficient accuracy was confirmed by repeating the calculations with finer and coarser grids; the results of these tests are shown in figure 3. The forward-step

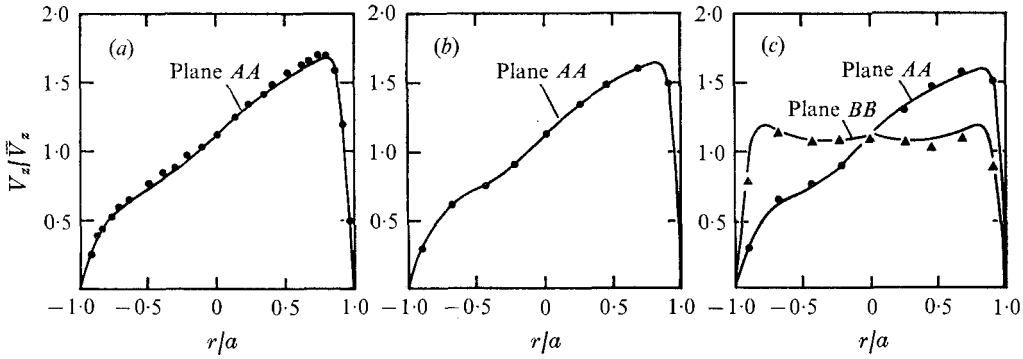

FIGURE 4. Comparison of axial velocity profiles with experimental data. (*a*) $K = 372{\cdot}0$, $R/a = 100$; ●, Adler (1934). (*b*) $K = 442{\cdot}7$, $R/a = 40$; ●, Mori & Nakayama (1965). (*c*) $K = 632{\cdot}4$, $R/a = 40$. ●, ▲, Mori & Nakayama (1965).

dependency was tested by repeating the computations with smaller and larger step sizes; a step size was then chosen which was small enough not to affect the solution. The developing-flow solutions were obtained by the marching procedure with small forward steps. However, when only the fully developed flow was to be computed, very large forward steps were taken and the velocities were under-relaxed at each step. The computer time needed to perform a developing-flow computation was of the order of 240 s on a CDC 6600 computer for 800 steps; the fully developed computation starting with a uniform velocity profile needed about 60 s for 140 steps.

3.2. *The flow field*

The computations of velocity profiles and friction factors in fully developed flow have been compared with the experimental data of various authors. Figure 4 compares the present predictions of the fully developed velocity profiles with those of Mori & Nakayama (1965) and Adler (1934). Figure 5 compares the corresponding friction factors with data of various authors (from Ito 1970). The agreement with experiment is very good. Figures 6–8 display the development of the velocity field along the z direction and comparisons with experimental data of Austin (1971). The agreement is quite good, considering the fact that the inlet velocity profiles in the experiment were not exactly parabolic.

The computed axial-velocity profiles at various angular planes are shown in figure 9, and figure 10 displays the effect of Dean number on the axial-velocity profiles. It can be seen that the velocity peak is shifted towards the outside as the Dean number is increased.

3.3. *Heat transfer*

The heat-transfer rates in helical coils are larger than the straight-tube value and have a wide peripheral variation. The present predictions of fully developed temperature profiles under the condition of axially uniform heat flux have been compared with experimental data of Mori & Nakayama (1965). Figure 11 shows

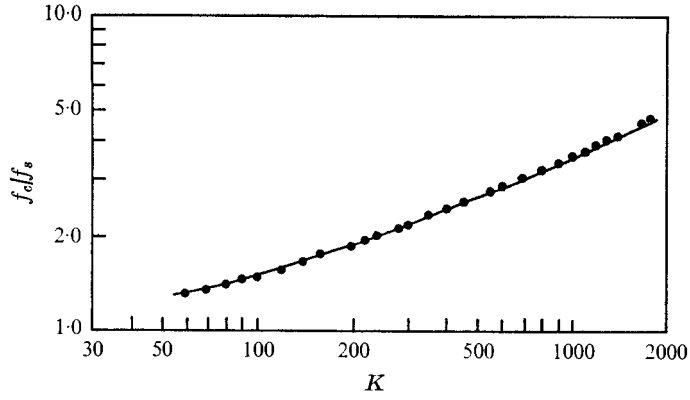

FIGURE 5. Comparison of fully developed friction factors f with experimental data. f_c and f_s are the curved-tube and straight-tube values respectively. ——, predictions; ●, Ito (1970).

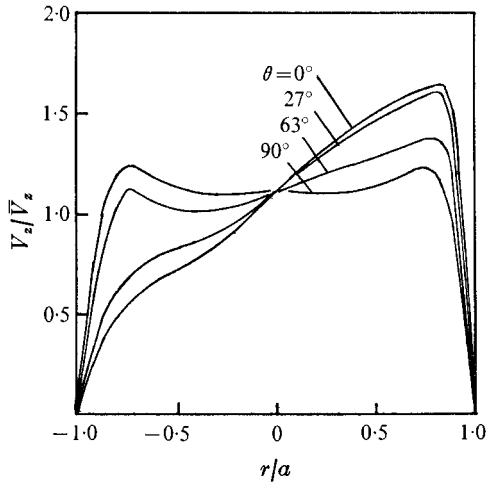

FIGURE 6. Axial-velocity field represented along various planes at $K = 442{\cdot}7$, $R/a = 40$.

good agreement in the outside half of the plane but there are significant differences in the inside region. Further comparisons have been made with the theoretical solution of Akiyama & Cheng (1971); from figure 12 it can be seen that there is good agreement in the range of Dean numbers which they considered. It is also observed that the inside heat-transfer coefficient approaches about half the straight-tube value at a Dean number of 300 and then increases slowly to the straight-tube value at a Dean number of 1200.

In contrast to the theoretical predictions, the experiments of Mori & Nakayama show much steeper temperature gradients on the inside. In view of the comparison in figure 12, it appears that their temperature profile may be in error, either owing to inaccuracy in measurement or imperfection in setting up the stated temperature boundary conditions.

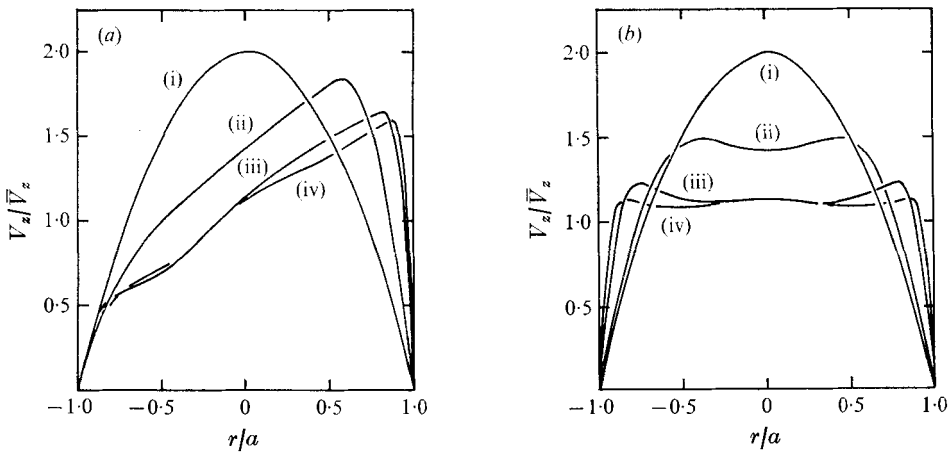

FIGURE 7. Effect of Dean number on axial-velocity profiles in (*a*) the plane AA and (*b*) the plane BB (see figure 2). (i) Straight tube. (ii) $K = 60{\cdot}0$. (iii) $K = 500{\cdot}0$. (iv) $K = 1200{\cdot}0$.

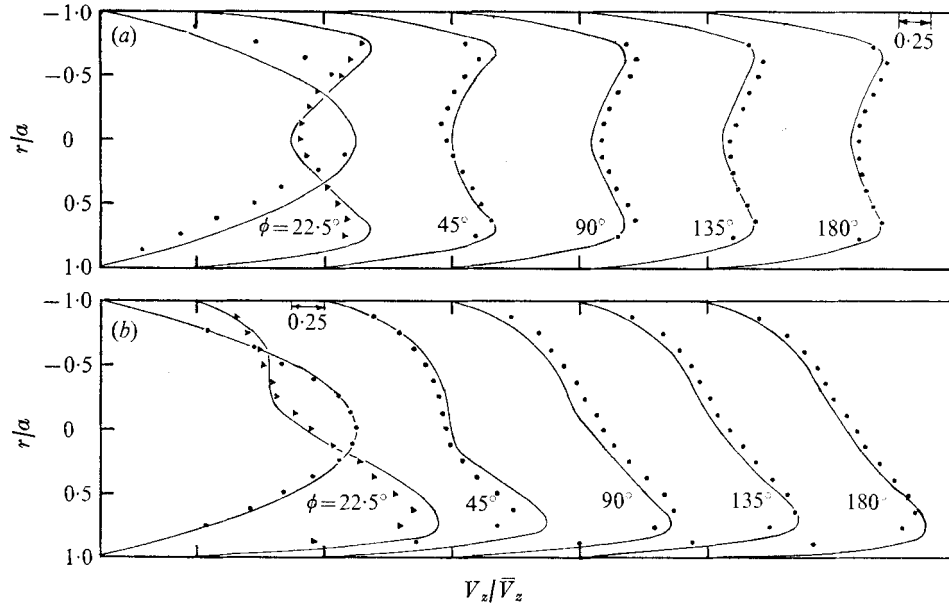

FIGURE 8. Development of axial velocity at $K = 198{\cdot}0$ and $R/a = 29{\cdot}1$ in (*a*) the plane BB and (*b*) the plane AA. ——, predictions; ●, ▲, Austin (1971).

Despite the discrepancy in temperature profile, the mean Nusselt numbers seem to be in good agreement as shown in figure 13(*a*). Figure 13(*b*) shows a comparison of our predictions for the fully developed Nusselt number with experimental data of Dravid (1971). In his experiments, the Prandtl number varied from 6 to 4 over the developing region. Since the comparison in figure 13(*b*) is for the fully developed condition, our computations were based on a uniform Prandtl number of 4, which was appropriate to the outlet condition. The effect of Dean number on the temperature profiles is shown in figure 14.

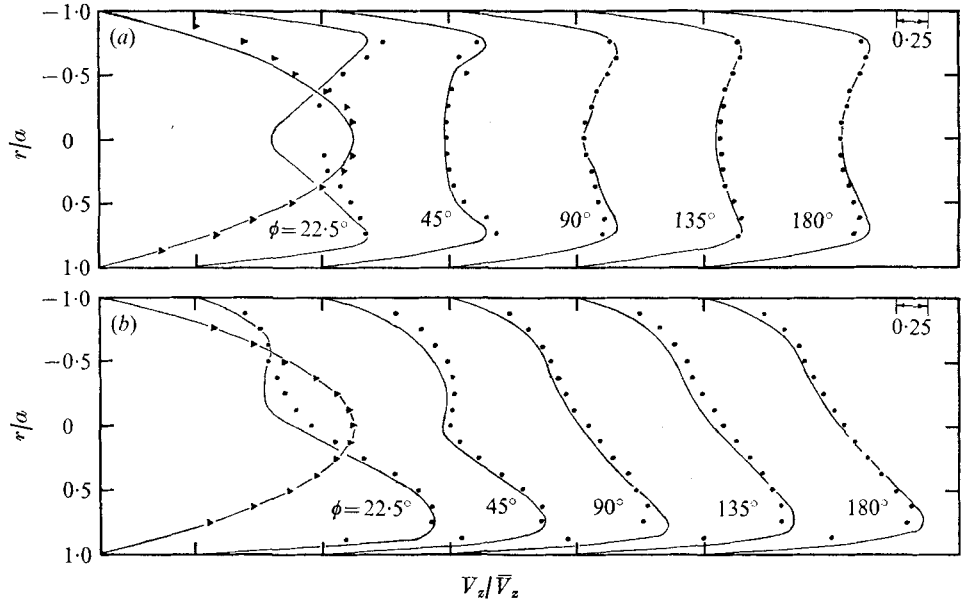

FIGURE 9. Development of axial velocity at $K = 280{\cdot}0$ and $R/a = 29{\cdot}1$ in (*a*) the plane BB and (*b*) the plane AA. Notation as in figure 8.

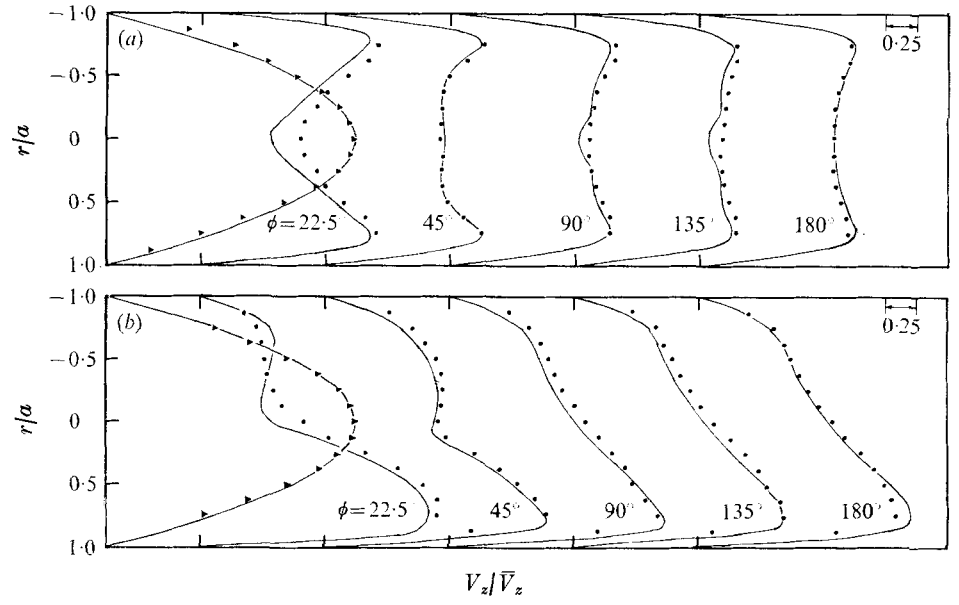

FIGURE 10. Development of axial velocity at $K = 372{\cdot}0$ and $R/a = 29{\cdot}1$ in (*a*) the plane BB and (*b*) the plane AA. Notation as in figure 8.

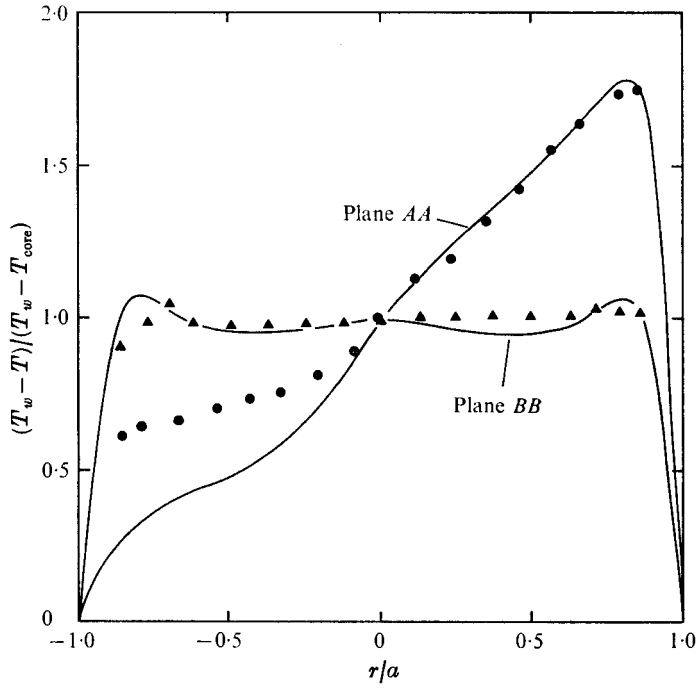

FIGURE 11. Temperature profiles along the planes AA and BB; $K = 632{\cdot}4$, $R/a = 40{\cdot}0$ and $Pr = 0{\cdot}71$. ——, predictions; ●, ▲, Mori & Nakayama (1965). T_w is the wall temperature.

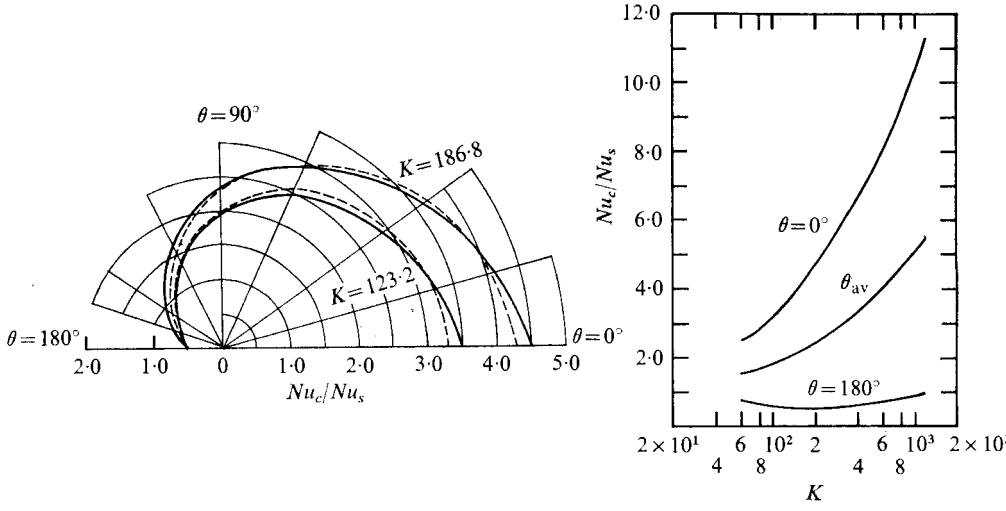

FIGURE 12. Local variation of Nusselt number Nu with Dean number. Nu_c and Nu_s are curved-tube and straight-tube values respectively; the curve marked θ_{av} gives values averaged over the periphery. $Pr = 0{\cdot}71$. ——, present results; – – –, Akiyama & Cheng (1971).

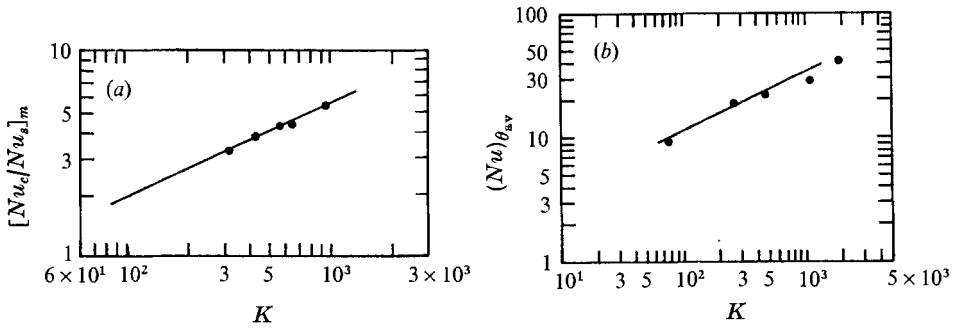

FIGURE 13. Variation of Nusselt number with Dean number. (*a*) Pr = 0·71. ——, predictions; ●, Dravid (1971). The subscript m indicates the mean value. (*b*) Pr = 4·0. ——, predictions; ●, Mori & Nakayama (1965).

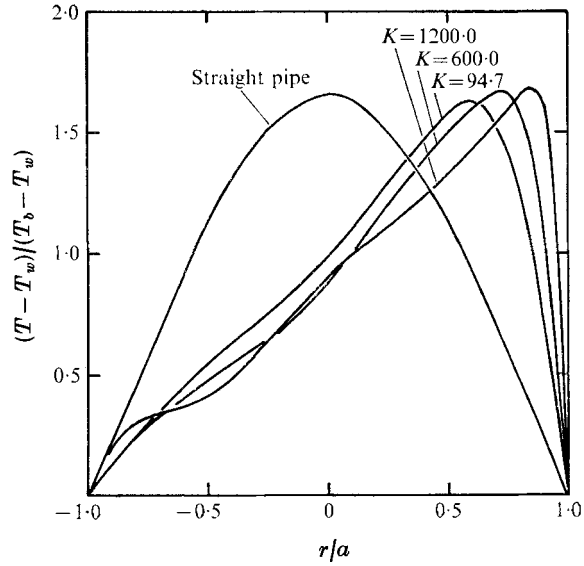

FIGURE 14. Effect of Dean number on the temperature profile along the plane AA; Pr = 0·71. T_b is the bulk temperature.

3.4. *The thermal entrance region*

The development of the temperature field was studied under the condition of axially constant heat flux with an isothermal periphery; the results are shown in figure 15. It was observed that the wall temperature exhibits cyclic oscillations, which are damped out as the fully developed thermal field is established. That the oscillations are not due to any numerical instability was confirmed by repeating the computations with different forward-step sizes. It was ascertained that the oscillations are a consequence of the secondary flow as had also been reported earlier by Dravid (1971) and Seban & McLaughin (1963).

The present predictions are compared with experimental results of Dravid (1971); the agreement is satisfactory although the predictions show a quicker

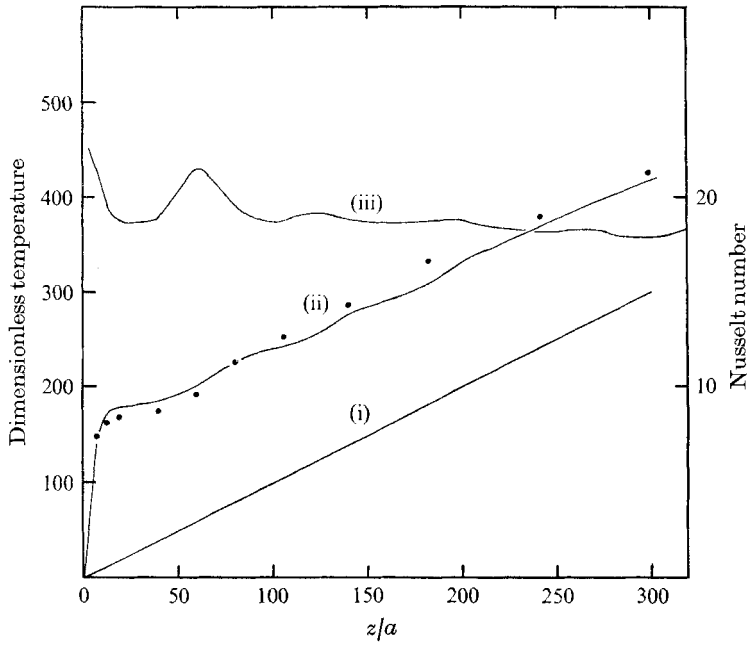

FIGURE 15. Development of wall temperature and Nusselt number for the case of axially constant heat flux at $K = 225{\cdot}0$ and $R/a = 20{\cdot}0$. (i) Bulk temperature. (ii) Wall temperature. (iii) Nusselt number. The non-dimensional temperature is $T/[\partial T_b/\partial(z/a)]$. ——, predictions; Dravid (1971).

	λ	
Dean number	Computed	Experimental
225.0	51·0	52·5
447.0	71·0	75·0
800·0	73·0	100·0

TABLE 1

damping of the oscillations. A dimensionless wavelength λ of the first oscillation, defined as the distance z/a between the point at which a line parallel to the bulk temperature line is tangential to the first maximum and first minimum in the wall-temperature curve, is compared with experimental results for various Prandtl and Dean numbers. The computations confirm the experimental results of Dravid that the Prandtl number, in the range studied (0·7–15·0), has little effect on the wavelength λ. Table 1 shows the wavelength λ for a few Dean numbers.

4. Conclusions

The method of Patankar & Spalding (1972) has been successfully applied to developing and to fully developed flow in coiled pipes. No numerical difficulties have been encountered and the computer times required are quite modest.

The predictions show very satisfactory agreement with available experimental data and theoretical solutions.

Further tasks are the following.

(i) Extension of the method to flows with small curvature ratio (R/a).

(ii) Incorporation of a turbulence model to predict the turbulent flow in curved pipes.

(iii) Application of the method to non-Newtonian flows which occur in physiological and other systems.

Work on these tasks is currently in progress.

The study was carried out with the financial support of the Science Research Council through a contract on three-dimensional duct flows. The computer program was developed by Dr S. V. Patankar with support from Combustion Heat and Mass Transfer Ltd. Mr A. Nigam assisted in the preparation of the figures. The authors wish to thank the above organizations and persons for their assistance.

REFERENCES

ADLER, M. 1934 Strömung in gekrümmten Rohren. *Z. angew. Math. Mech.* **14**, 257.

AKIYAMA, M. & CHENG, K. C. 1971 Boundary vorticity method for laminar forced convection heat transfer in curved pipes. *Int. J. Heat Mass Transfer* **14**, 1659.

AUSTIN, L. R. 1971 The development of viscous flow within helical coils. Ph.D. thesis, University of Utah.

CARETTO, L. S., CURR, R. M. & SPALDING, D. B. 1971 Two numerical methods for three-dimensional boundary layers. *Imperial College, Mech. Engng Rep.* EF/TN/A/40.

DEAN, W. R. 1927 Note on the motion of fluid in a curved pipe. *Phil. Mag.* **14**, 208.

DRAVID, A. N. 1971 Effect of secondary fluid motion on laminar flows and heat transfer in helically coiled tubes. *A.I.Ch.E. J.* **17**, 1107.

ITO, H. 1970 Laminar flow in curved pipes. *Rep.* no. 224. *Inst. High Speed Mech., Japan*, vol. 22, p. 161.

MCCONALOGUE, D. J. & SRIVASTAVA, R. S. 1968 Motion of a fluid in a curved tube. *Proc. Roy. Soc.* A **307**, 37–53.

MORI, Y & NAKAYAMA, W. 1965 Study on forced convective heat transfer in curved pipes (1st report, Laminar region). *Int. J. Heat Mass Transfer*, **8**, 67.

PATANKAR, S. V. & SPALDING, D. B. 1972 A calculation procedure for heat, mass and momentum transfer in three-dimensional parabolic flows. *Int. J. Heat. Mass Transfer*, **15**, 1787.

SEBAN, R. A. & MCLAUGHIN, E. F. 1963 Heat transfer in tube coils with laminar and turbulent flow. *Int. J. Heat Mass Transfer*, **6**, 387.